Contactless Surface Registration of Featureless Anatomy using Structured Light Camera: Application to Fibula Navigation in Mandible Reconstruction

Lénaïc Cuau[1*], Marie De Boutray[1,2], João Cavalcanti Santos[1], Nabil Zemiti[1] and Philippe Poignet[1]

[1]LIRMM, University of Montpellier, CNRS, Montpellier, France.
[2]Department of Maxillofacial Surgery, Gui de Chauliac University Hospital, Montpellier, France.

*Corresponding author(s). E-mail(s): lenaic.cuau@lirmm.fr;
Contributing authors: m-deboutray@chu.montpellier.fr;
joao.cavalcanti-santos@lirmm.fr; nabil.zemiti@lirmm.fr;
philippe.poignet@lirmm.fr;

Abstract

Purpose Mandibular reconstruction using fibula free flap is a challenging surgical procedure. To assist osteotomies, computer assisted surgery (CAS) can be used. Nevertheless, precise registration is required and often necessitates anchored markers that disturb the patient and clinical flow. This work proposes a new contactless surface-based method adapted to featureless anatomies such as fibula to achieve a fast, precise and reproducible registration.
Methods Preoperatively, a CT-scan of the patient is realized and osteotomies are virtually planned. During surgery, a structured-light camera digitizes the fibula. The obtained intraoperative point cloud is coarsely registered with the preoperative model using 3 points defined in the CT-scan and located on the patient's bone with a laser beam. Then, a fine registration is performed using an ICP algorithm. The registration accuracy was evaluated comparing the position of points engraved in a 3D-printed fibula with their position in the registered model and evaluating resulting osteotomies.

Accuracy and execution time were compared to a conventional stylus-based registration method. The work was validated in-vivo. **Results** The experiment performed on a 3D-printed model showed that execution time is equivalent to surface-based registration using a stylus, with a better accuracy (mean TRE of 0.9 mm vs 1.3 mm using stylus) and guarantee good osteotomies. The preliminary in-vivo study proved the feasibility of the method. **Conclusion** The proposed contactless surface-based registration method using structured-light camera gave promising results in terms of accuracy and execution speed and should be useful to implement CAS for mandibular reconstruction.

Keywords: mandibular reconstruction, surface-based registration, structured-light scanner, fibula

1 Introduction

Mandibular reconstruction using fibular free flap (FFF), as described by Hidalgo in 1988, is a standard procedure in maxillo-facial surgery [1]. The FFF is a bone autograft taken on the patient's fibula and shaped to reconstruct the length and form of the mandible. Despite the potential benefits of this type of surgery, achieving the osteotomies to shape the fibula may be challenging and time-consuming. The surgeon must cut the fibula into several fragments that should fit among themselves to reconstruct an aesthetic and functional mandible [1]. Accordingly, freehand FFF is an intervention that demands extensive experience (60 to 100 flaps) to obtain a reasonable success rate (95 %) [2]. To overcome this difficulty, patient-specific instrumentation (PSI) is frequently used by surgeons. Based on preoperative imaging, a patient-specific guide is designed to constrain the positioning of the saw on the fibula. However, these guides are expensive, long to produce (3 to 6 weeks) and the surgical planning can not be modified during the surgery in case of a tumor progression [3].

That is why computer assisted surgery (CAS) could offer a valuable solution to help FFF osteotomy positioning. CAS has expanded over the years and is now commonly used in orthopedic surgery. CAS has been shown to improve functional outcomes compared to conventional operation [4]. In maxillofacial surgery, and more specifically reconstructive mandibular surgery, CAS is not frequently used while there would be a real interest in developing such techniques [5, 6, 7, 8]. Recently, navigation has been used for mandibular shape reconstruction guidance [5] and to guide osteotomies [6]. Robotic assistance has also been proposed in the literature to place previously cut fragments [8] or automatically perform the osteotomies based on planning [7]. Although these studies led to encouraging results, they require a precise

registration process as the desired precision in this surgical application within the literature is 2 mm [6].

Artificial markers are the gold standard for this registration but imply many drawbacks such as patient discomfort and hospital flow complications. Surface-based registration methods are thus preferred. They aim to register the preoperative patient's bone surface data extracted from a CT-scan volume with the corresponding intraoperative surface data digitized with a navigated tracked stylus. However, using a tracked stylus for surface digitization is not always accurate because of its calibration precision and tissue deformation upon contact. Moreover, for large surface acquisition, it is time-consuming and user dependent [9]. Camera-based solutions (laser range scanner, time-of-flight cameras, structured-light cameras, etc.) for patient's bone surface digitization have become quite common in CAS since they are faster, contactless, and have fewer sterilization constraints than tracked stylus [10, 11, 12]. They can acquire thousands of points in a few seconds without any contact. These advantages inspired the application of laser range scanners in neurosurgery [10] or knee arthroplasty [11]. All those registration processes are based on the detection of specific features (anatomical [12] or screwed[10]), or shape characterization [11] to make a coarse registration and then refine it with an iterative closest point (ICP) algorithm. Nevertheless, in our context, the surface of the bone to be registered (the fibula) is featureless and cylindrically symmetric. Thus, a surface-based registration method as proposed in [10, 11, 12] cannot be applied. Therefore, in the context of mandibular reconstruction, artificial markers are predominantly used [7, 8], which unfortunately present, as mentioned before, many drawbacks.

To solve registration issues related to surfaces lacking specific features and characteristic shapes without introducing artificial markers nor using a tracked stylus, this work proposes a surface-based registration method using a structured light camera initialized by point matching. These keypoints are created and located by the surgeon on the CT-scan volume and defined in the surgically exposed area to be detected in the intraoperative image. The combination of this point matching initialization and dense surface acquisition can achieve a fast, precise, reproducible, and contactless rigid registration of the fibula. To the best of our knowledge, this is the first time a structured-light camera has been used to register a featureless bone as the fibula. The accuracy of the proposed method has been evaluated on a 3D-printed fibula model, and its feasibility has been evaluated on a human patient leg. The main contributions of this paper are: (1) The proposition of a contactless surface-based rigid registration method using a structured-light camera for featureless anatomy and (2) its validation in the context of mandibular reconstruction.

The content of this paper is organized as follows: first, the material and methods used are presented section 2 by giving an overview of the system

and detailing the camera calibration method and the registration process. Then, experiments performed on the 3D-printed fibula and the human leg are presented section 3. The obtained results are discussed in section 4. Finally, conclusions are drawn in section 5.

2 Material and methods

This work aims to localize the planned osteotomies on the fibula in the OR by finding the transformation between the CT-scan, where the osteotomies were planned, and the patient in the OR. To do so, a structured-light camera is used to acquire the patient's fibular surface (noted $\mathcal{B}_C$ in the following). By registering this acquisition with the CT-scan volume, the desired transformation is found. The surgeon can then be guided through augmented reality, navigation, or physical constraints positioned by a robot.

2.1 System overview

The system has two main devices (Fig.1). The first one is an optical tracking system (FusionTrack 500 from Atracsys) able to detect and localize passive markers that reflect infrared light. It was used in this work to detect markers fixed on the camera and on the bone to localize them in the same coordinate system. In a real scenario, it is placed in the OR and considered as the main reference frame. The artificial marker on the bone is not used for registration but only for tracking in case of bone movement. A calibration step is necessary to establish the transformation between the camera and its marker (see section 2.2).

The second device is the camera Surface HD 20 (Revopoint). Its optimal working distance is 200±50 mm. It uses binocular infrared structured light and does not give RGB information. It has been used to produce a dense point cloud of the bone surface that has been registered with the CT-scan volume. The different data were treated with Point Cloud Library (PCL, https://pointclouds.org/).

Fig. 1 Set up for optical palpation of the fibular bone using structured-light camera and localisation in the operating room using an optical tracking system

2.2 Camera Calibration

Let, for A and B be two frames, ${}^{A}T_{B}$ be the transformation from B to A and W, C, and M_c, be respectively the frames attached to the world (localizer considered as the OR frame), the camera, and the marker on the camera (fixed to it with a 3D printed support as in Fig.1). The calibration of the camera consists in the determination of ${}^{C}T_{M_c}$, which is then used to express the acquired point cloud in W with $\mathcal{B}_W = {}^{W}T_{M_c}.({}^{C}T_{M_c})^{-1}\mathcal{B}_C$. Although techniques using chessboards are frequently used for RGB camera calibration [13], the 3D measurements obtained with an RGB-D camera can be used to achieve improved precision [14, 15, 16]. In this case, a volumetric calibration phantom is adopted. Accordingly, the automatic 3D calibration method introduced in [15] was applied with the phantom depicted in Figure 2. The phantom was conceived to be as simple as possible: a cube with a marker fused to it to reduce the deformation as much as possible and cubic shapes on its faces to have precise registration (Fig.2). Let P and M_p be the frames attached to the calibration phantom and its marker respectively. The goal was to compute the transformation ${}^{C}T_{M_c}$ via Eq.1.

$$ {}^{C}T_{M_c} = {}^{C}T_{P}.{}^{P}T_{M_p}.{}^{M_p}T_{W}.{}^{W}T_{M_c} \tag{1} $$

The different members of Eq.1 can be solved separately: ${}^{C}T_{P}$ is computed with an ICP registration of the CAD model expressed in P with the point cloud generated by the camera expressed in C. ${}^{P}T_{M_p}$ is known by CAD model of the calibration phantom. ${}^{M_p}T_{W}$ and ${}^{W}T_{M_c}$ are given by the optical tracking system. This method has the advantage to be simple (it only requires the design and printing of the phantom), fast (on average 40 s) and does not necessitate any experience from the user.

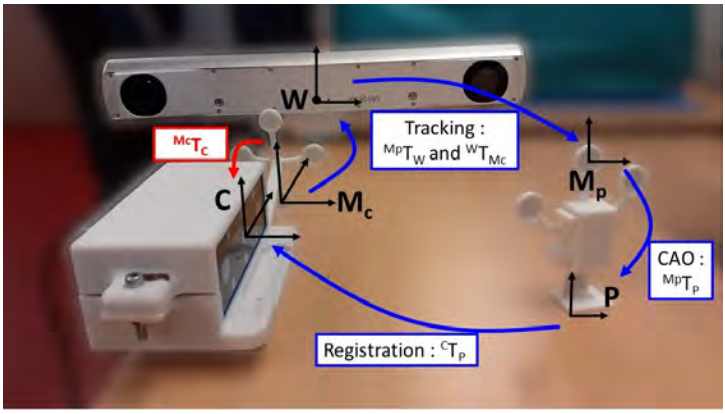

Fig. 2 Setup used for camera calibration : camera observes the calibration object and the algorithm registers this acquisition with the CAD model

2.3 Registration

To register the fibular data in the physical space (localizer frame) with the fibula CT-scan volume, a marker-free point cloud registration was performed. Firstly, a rough registration is performed based on 3 non-aligned initialization points. Afterwards, a precise registration is applied based on 20,000 points obtained with the RGB-D camera.

As with every other FFF harvesting surgical procedure, the fibula will be exposed and pulled back from the leg by cutting its two extremities which need to remain attached to the tibia to ensure the stability of the ankle. The lower two-thirds of the exposed fibula will be used for mandible reconstruction, so it has to remain coated by muscle and vessels to be revascularized once transferred to the mandible. The remaining part (the upper third), which will not be used for the surgery, can be stripped, digitized, and used for registration (Fig. 3). Thus, only a subset of the acquired point cloud, chosen via a user interface, will be used for registration. In general (depending on the length of the region of interest) 20,000 points are captured with 0.04 mm spacing in 50 ms. Once the camera is calibrated w.r.t to the marker attached to it, the bone surface is acquired in W: $\mathcal{B}_W = {}^{W}T_{M_c}.{}^{M_c}T_C.\mathcal{B}_C$.

To rigidly register $\mathcal{B}_W$ with the CT-scan volume, the ICP standard algorithm [17] is used. As the exposed part of the fibula presents a geometry close to the cylinder, a suitable ICP initialization is required. The initialization was done with three non-aligned points. Three points are defined by the surgeon on the CT-scan volume via a mesh editing software (CloudCompare, www.cloudcompare.org) before the operation $\{{}^{CT}P_i\}_{i=1:3}$. Those points have to be non-aligned and can be chosen anywhere on the bone. We have chosen to place two of them on the ridge of the fibula and one on the face to facilitate their placement in the real fibula. The first point P_1 was defined on the posterior ridge of the fibula, at a chosen distance d_{01}=10 cm from the distal extremity of the malleolus M. The second point P_2 was defined on the middle of the lateral face of the fibula at a chosen distance $d_{12} = 3$ cm from P_1. The third point P_3 was defined on the posterior ridge of the fibula at a chosen distance $d_{13} = 2.5$ cm from P_1.

During the operation, and before cutting the malleolus, the surgeon finds these three points with a ruler (thanks to their distance to the malleolus and their localization on the ridges or face of the fibula) and draws them with a surgical marker pen. The fibula is then pulled back from the leg and stripped on the upper third. The marks cannot be detected in the point cloud that has no color, so the user directs the beam of a common laser pointer toward these reference points. The laser beam generates a hole in the point cloud by disturbing the projected pattern, so the camera cannot deduce the depth of this zone. This point cloud with the hole is subtracted from the entire point cloud to obtain a set of points that approximately forms a disk of center

$\{^{W}P_i\}_{i=1:3}$. A coarse registration is performed with the two sets of points $\{^{CT}P_i\}_{i=1:3}$ and $\{^{W}P_i\}_{i=1:3}$. The ICP is then executed to perform the fine registration between $\mathcal{B}_W = \{p_1, ..., p_n\}$ and $\mathcal{B}_{CT} = \{q_1, ..., q_m\}$ by minimizing $E(R,t) = \sum_{i=1}^{n} \|(Rp_i + t) - q_j\|$ with (p_i, q_j) a pair of corresponding points with $j = argmin_{1 \leq k \leq m} \|p_i - q_k\|$. The pairs (i,j) are updated taking a new set $B'_W = \{R.p_1 + t, ..., Rp_n + t\}$. The procedure is repeated until $E(R,t) < 0.01$ mm.It results in the final transformation $^{CT}T_W$ and planned osteotomies on the CT-scan volume are then expressed in the world frame.

Finally, it is important to note that the fibula has to remain attached to the vascular pedicle during the surgery and can move. That is why a disposable or sterilizable tracked marker is rigidly fixed on the bone at the beginning of the surgery. Thus, the planned osteotomies poses can be updated in real-time via the localizer acquisition. This procedure does not lead to any issues since the marker is fixed during the surgery and on the proximal extremity of the exposed fibula which will not be used for the reconstruction (Fig. 3).

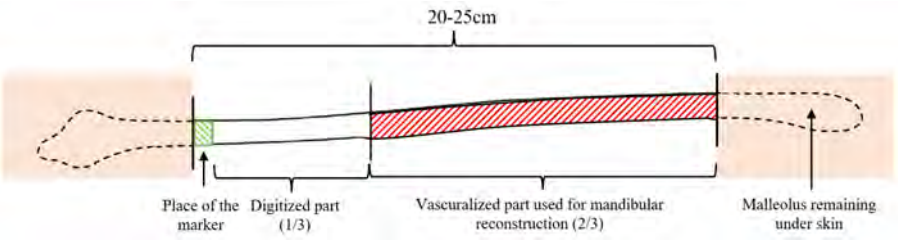

Fig. 3 Schematic representation of the fibula bone and the parts used for registration and mandibular reconstruction.

3 Experiments and results

To assess the performance of the proposed calibration and registration methods, the calibration precision was validated with a reference 3D-printed model. Then, the registration precision was assessed on a 3D-printed fibula. Its performance was compared in terms of time and precision with a manual palpation method using a tracked stylus. Finally, a proof of concept on a patient in an OR was performed.

3.1 Camera calibration

To evaluate the precision related to the camera calibration, a 3D-printed object was used as reference geometry. It consists of a marker with a cube, in a single piece, with some holes, detectable by the camera, placed at known localizations w.r.t. the marker frame (M_o): $\{^{M_o}P_i\}_{i=1:3}$. This object was 3D-printed in PolyLactiq Acid (PLA) via a 3D desktop printer (Ultimaker s3, 0.01 mm layer thickness, 0.78 mm positioning resolution on the X/Y axis). The calibration

precision is then expressed as the error $\|{}^{C}P_i - {}^{C}T_{M_c}.{}^{M_c}T_W.{}^{W}T_{M_o}.{}^{M_o}P_i\|_{i=1:3}$. On 25 calibrations procedures, the mean error was 0.3 ± 0.2 mm, with a maximum of 0.8 mm and minimum of 0.1 mm.

3.2 Results on 3D-printed model

3.2.1 Registration accuracy

The precision of the registration method was evaluated on a 3D-printed fibula. The fibular model was created from a preoperative CT-scan (resolution 710x710x625 mm3) of a human leg. The DICOM images were segmented manually with 3D Slicer software to generate a 3D mesh. Five assessments points noted $\{{}^{CT}M_i\}_{i=1:5}$ and represented by holes (Ø 1 mm) were defined in the model. An attachment for the marker was added to the model, its associated frame is noted M_b. This 3D fibular model with holes and marker fixation was 3D printed with the same parameters listed in section 3.1. The holes were visible on the 3D-printed fibula. The registration process is performed with the upper one-third of the bone (see section 2.3) and gives ${}^{W}T_{CT}$.

To evaluate the accuracy of the procedure, the "ground truth" positions of the assessment points $\{{}^{W}M_i\}_{i=1:5}$ are obtained by positioning a calibrated [18] tracked stylus within the holes. For each M_i the Target Registration Error (TRE) $\|{}^{W}T_{CT}.{}^{CT}M_i - {}^{W}M_i\|_{i=1:5}$ is computed along the three principal axis (**x**,**y**,**z**) of the fibula computed with Principal Component Analysis (PCA) (Fig.4).

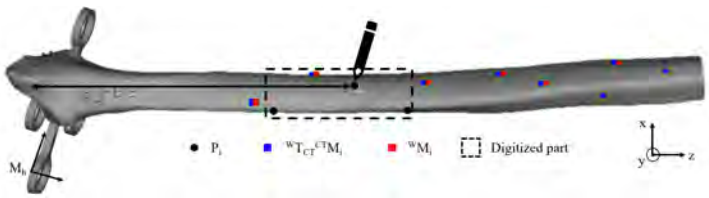

Fig. 4 Registration initialization and assessment: Initialization points definition (in black) and surface scanning are done on the distal third of the fibula. Points used for precision assessment are registered (blue points) and detected with a tracked stylus (red points)

Ten procedures were performed with the same 3D-printed bone and the same operator. At each time the camera and the stylus were re-calibrated. A TRE of [0.5±0.1 ; 0.4±0.04 ; 0.9±0.1] mm along the **x**-, **y**- and **z**-axis respectively was obtained. The mean standard deviation (SD) of the distance within the points was 0.2±0.1 mm. Errors are reproducible given the SD of 0.2 mm within the procedures.

A comparative study was performed with a manual registration technique that can also be adapted to the homogeneity of the fibula, which consists of gathering surface information with a tracked stylus [9]. The same operator did

manual palpation and optical palpation ten times each. The goal was to evaluate the global execution time, the registration precision, its repeatability, and the dependency on the user experience of each method. Concerning execution time, initialization and palpation with the stylus took, on average, 2.8±0.4 min. Laser initialization and optical scanner took 2.5±0.4 min, representing a 10% reduction in the average lead time. Regarding accuracy, for the stylus, a TRE of [0.5±0.1; 0.5±0.2;1.3±0.03] mm was observed along **x**-, **y**- and **z**-axis, which is higher than results with the camera ([0.5±0.1; 0.4±0.04; 0.9±0.1]). Figure 5 summarises these results.

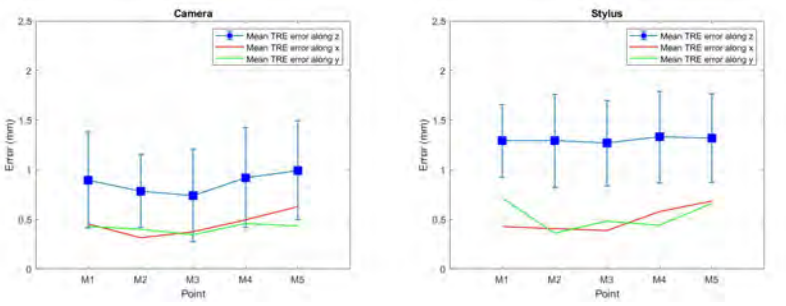

Fig. 5 TRE along the principal axis of the fibula for the 5 assessment points for registration with optical (left) and manual (right) palpation made 10 times

3.2.2 Cutting results

Even if a low TRE is satisfying and means that the registration is acceptable, it is not entirely relevant because a slight homogeneous error on all the assessment points along the axis of the fibula has no clinical consequence on the cutting of the fibula since it is nearly cylindrical. Fibula cutting was thus simulated to evaluate the impact of registration error on final osteotomies. Two slots were defined in the CT scan as 3D planes, and transformed with the rotation and translation between ${}^{CT}M_i$ and ${}^{CT}T_W.{}^{W}M_i$ (defined and acquired assessment points). The resulting slots were then used to virtually cut the fibula CT-scan. The obtained fragments were compared to the planned one using cloud-to-cloud distance. The mean maximum difference was 0.1±0.02 mm and 0.2±0.06 for camera and stylus-based registration respectively.

3.2.3 Sensitivity to initialization

The accuracy of the proposed method relies heavily on the initialization step, which is an inherent issue of the ICP algorithm. To investigate the impact of initialization point placement on the final result, 200 simulations of their placement were conducted. Let $\{P_i = (x_i, y_i, z_i)\}_{i=1:3}$ be the three ideal initialization points in the fibula's frame (**x**,**y**,**z**) as defined in Fig. 6. Let d_{12}=$P_1P_2.z$

and $d_{13} = P_1P_3.z$. Those two distances are previously chosen by the surgeon on the CT-scan as explained in section 2.3. The three simulated real initialization points $\{\hat{P}_i\}_{i=1:3}$ positioned on the real fibula were thus defined as follows:

- In clinical practice, P_1 is defined on the posterior ridge of the fibula thanks to the distance d_{01} from the distal end of the malleolus M. The estimation of M by palpation introduces a ± 10 mm error on P_1 position along the ridge of the fibula resulting in $\hat{P}_1 = (\hat{x_1}, \hat{y_1}, \hat{z_1}) = (x_1, y_1, z_1 \pm 10 \text{ mm})$. We assume there is no error on x and y axis since the point is placed on the posterior ridge.
- P_2 is defined at a given distance d_{12} from P_1 on the middle of the lateral face of the fibula. We assume that when the user measure the distance from $\hat{P}_1$ with a surgical ruler, the introduced error on P_2 position along the bone axis is $\pm$ 2 mm. In addition, since P_2 is located on the middle of the lateral face of the fibula,an error along x-axis could also appear and was assumed to be $\pm$ 3 mm. That is to say, $\hat{P}_2 = (\hat{x_2}, \hat{y_2}, \hat{z_2}) = (x_2 \pm 3 \text{ mm}, y_2, \hat{z_1} + d_{12} \pm 2 \text{ mm})$.
- P_3 is placed on the posterior ridge of the fibula based on the placement of P_1. As for P_2, we assume that when the user measure the distance from $\hat{P}_1$ with a surgical ruler, the introduced error along the bone axis is $\pm$ 2 mm which gives $\hat{P}_3 = (\hat{x_3}, \hat{y_3}, \hat{z_3}) = (x_3, y_3, \hat{z_1} + d_{13} \pm 2 \text{ mm})$. We also assume that there is no error on x and y axis since the point is placed on the posterior ridge.

The three points were randomly uniformly distributed in their position range and the TRE and resulting fragments were evaluated (Fig. 7). Mean TRE along **x**-, **y**- and **z**-axis were [2.0$\pm$0.1, 1.0$\pm$0.1,4.6$\pm$0.03] mm. It is interesting to note that the correlation coefficient between the z error and the distance of the first point from the malleolus was 0.98. Finally, as expected, this error on the **z**-axis has no prohibitory consequence on the osteotomies with mean of maximum fragment difference of 0.8$\pm$0.5 mm and maximum of 1.9 mm.

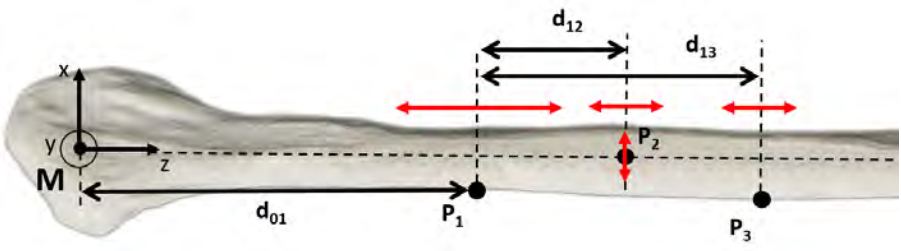

Fig. 6 Placement of the three initialization points : P_1 is placed on the ridge of the bone at a distance d_{01} from the malleolus, P_2 is placed on the face of the bone at a distance d_{12} from P_1 and P_3 is placed at a distance d_{13} from P_2.

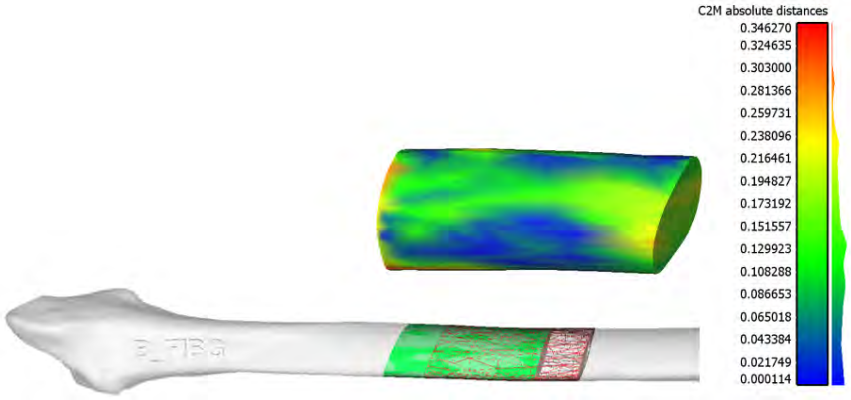

Fig. 7 Distance map of obtained fragment vs. planed fragment. Even if the fragment is translated along the fibula, its shape remains the same.

3.3 In-vivo feasibility

The in-vivo feasibility of the method was evaluated on a patient who needed fibula free flap to be raised. This study was done in order to validate the compatibility of the method with the real application, and identify major potential issues related to the OR environment (sterility, operating room footprint, specular reflections, blood, surgical workflow ...). There were no markers and no localizer in the OR so, as a preliminary part, we tested if the point cloud acquired on a real fibula is consistent and allowed us to perform the registration. To do so, firstly, two sets of three points were defined on the CT-scan at fixed distances from the malleolus and on edges of the fibula: $\{^{CT}M_i\}_{i=1:3}$ for precision assessment and $\{^{CT}P_i\}_{i=1:3}$ for ICP initialization. Secondly, the 6 points were coarsely marked on the fibula using a surgical pen by measuring the distances to the malleolus located under the skin. The fibula was then cut and pulled back from the leg. The camera was placed at about 30 cm from the patient as in Fig. 8 and the bone was scanned to get a point cloud on the area without muscle and periosteum thanks to the user interface. Then, the registration was performed after initialization with the P_i, as explained in section 2.3, to get $^{C}T_{CT}$. To evaluate that transformation, the TRE $\|^{C}T_{CT}.^{CT}M_i - ^{C}M_i\|_{i=1:3}$ was computed. The observed assessment points $^{C}M_i$ were determined with the laser pointer. The distances between the observed and the registered assessment points were 1.9, 1.7, and 3.6 mm.

4 Discussion

The aim of this work was to propose a fast, precise, reproducible, and contactless fibular registration method to achieve computer assisted osteotomies for mandibular reconstruction. The state-of-the-art in mandibular reconstructive surgery proposes free hand osteotomies, which have a success rate of 79% during the surgeon's early career that become reasonable (95 %) only

Fig. 8 Optical palpation of the fibula in an operatory room at Department of Maxillofacial Surgery, Gui de Chauliac University Hospital, Montpellier, France (Left). Bone registered with assessment points registered (blue) and detected with the laser (red)

for experienced surgeons (60 to 100 flaps) [2]. PSI can also be used but are expensive and have to be printed for each patient. In contrast, despite the significant initial investment necessary to use augmented reality, navigation, or robotic assistance, it presents low operating cost (a medico-economic study has to be done to assess this statement). It necessitates a precise registration process and it is clear that a surface-based registration method, which does not use fiducial markers placed on the patient before imagery, is beneficial in terms of patient comfort and hospital flow. However, for a featureless and cylindrical bone, this process could be difficult. Torres et al. [12] presented a work on the femur which is similar in shape to the fibula but they used ultrasounds and could detect the malleolus that has distinguishable features. In our work, malleolus is cut before the registration process thus cannot be used. We have shown in a previous work [9] that, in the case of the fibula, using a tracked stylus is possible but necessitate a trained surgeon. In this work, we have shown that using dense surface acquisition by a 3D camera, combined with point matching initialization, can perform a more precise registration, without artificial markers, adapted to the featureless bones such as the fibula.

The structured light camera allows dense information acquisition, which permits more accurate registration. Indeed, a more scattered point cloud leads to more significant registration errors: for the same initialization, the difference in the osteotomies generated by registration with a cloud of 20,000 points is 1 mm against 3.1 mm for a cloud of 500 points uniformly downsampled from the original set (more results are given in Table 1).

The proposed method's accuracy was evaluated on a 3D-printed fibula. The mean of maximum osteotomies difference was 0.1 mm which is under the precision requested in this surgical application within the literature (2 mm) [6]. The mean TRE for each point was [0.5±0.1;0.4±0.04;0.9±0.1] mm along $\mathbf{x}$, $\mathbf{y}$ and $\mathbf{z}$ which shows that the registration process is accurate. These results also means that the major error is along the bone axis as expected and is reproducible given the standard deviation within procedures. However,

Table 1 Maximum distance between cutted and planned fragments with respect to the number of points in the point cloud used for registration.

Number of points	Max distance (mm)
100	5.5
500	3.1
1000	2.5
5000	2.3
10000	2.2
20000	1.0

there is a non-negligeable error along **x** and **y** which could be explained by a non exact definition of (**x**,**y**,**z**) since the fibula is not stricly linear and has a small curvature.

Surface-based registration with a tracked stylus is a standard method in orthopedic surgery. This technique was used as a reference method to be compared with the contactless proposed method using structured light. The stylus method leads to a maximum error on fragments of 0.2±0.06mm, which is similar to the camera method. TRE value on assessment points of 1.26 mm is thus acceptable but less precise than the camera-based registration method (TRE = 0.9 mm). Besides, the mean TRE of the stylus-based method varies from 0.6 mm to 1.8 mm with an SD of 0.4 mm. This shows that this method lacks reproducibility as it is visible on the box whisker plot (Fig. 5). In contrast, the optical method is more reproducible within the procedures since global TRE is 0.9±0.2 mm. Furthermore, with the stylus-based method, TRE decreases progressively when the same user performs the procedure ten times. This shows that this method requires a longer learning curve from the user in contrast with the optical method where the mean TRE is approximately constant. However, more procedures with different operators have to be done to observe a statistically significant learning curve. Concerning execution time, even if for point cloud acquisition the camera is faster than the stylus (50 ms vs 2 min), initialization with the laser beam, region of interest selection, and camera placement necessitate 2.5±0.4 min that represents a 10% reduction in the average time compared to the stylus. That is beneficial but not significant w.r.t the surgery time. That could be improved using for instance the RGB part of an RGBD camera to automate the identification of the initialization points.

An inherent issue of the used registration algorithm (ICP) is its sensitivity to initialization. To handle this, three initialization points were used to perform coarse registration, which ICP then refines. However, the location of those points varies according to the surgeon's experience, especially when evaluating the distance from the malleolus. We simulated this variability 200 times and showed that even if the final TRE was linearly correlated with the first point placement, this did not impact the final osteotomies (mean difference of

0.8 mm between planed and performed osteotomies).Therefore, the introduced methodology benefit from the simplicity, accuracy and speed obtained with the ICP algorithm without being prone to its main drawback. Clearly, more elaborate approaches (e.g. learning-based [19], probabilistic-based [20] and other ICP-based methods [21, 22]) could be applied. Nevertheless, this would come with the expense of an additional complexity of the overall method. This aspect should be considered in future works and it is considered out of the scope of the present paper.

The method feasibility was validated in the OR by acquiring a point cloud and registering it with the CT-scan volume. This part of the validation, although preliminary with respect to the assessment of precision, is relevant as a feasibility evaluation in surgery. It showed that registration in the OR is possible and does not disturb the surgery workflow. It also provided an estimation of the registration accuracy (average of 2.3 mm) which, even if greater than 2 mm, remains acceptable given the evaluation method itself. Indeed, it has to be noted that this evaluation method has to be considered carefully since each assessment point was only acquired once due to a lack of time in the operating theatre. Besides, when aiming to a point, the center of the laser beam never accurately corresponds to the real point coordinates because of the size of the spot and human eye precision. The accuracy of the points localization with this laser is in mean 0.8 mm with high in-plane SD (σ_x=0.6 mm, σ_y=0.7 mm, σ_z=0.1 mm). It was computed by pointing to a known point engraved in a 3D piece 50 times and computing $\| {}^{W}T_{M_o}.{}^{M_o}P - {}^{W}T_{M_C}.{}^{M_C}T_C.{}^{C}P \|$ with M_o the frame attached to the marker on the 3D piece.

Some limitations still have to be studied in future works. First, the location of the malleolus under the skin could be hard to recover from in overweight or traumatized legs and necessitates the use of an intraoperative ultrasound scanner. Secondly, stripping the bone from the muscles and periosteum is time-consuming. Moreover, finding and drawing initialization points requires some time. Global optimization algorithms (that could require more time for convergence) should then be studied to assess if they can deal with the cylindrical shape of the fibula without an initialization step. The time required for initialization (or convergence) still has to be balanced with the conventional flap harvesting time which is 50 to 125 min [23]. The registration process was evaluated at 2.5 min but the global procedure time with navigation or robotic assistance has to be studied. Finally, the proposed registration method can be used for different types of CAS: augmented reality, navigation, or robotic assistance. However, the setup is cumbersome as it necessitates the use of a localizer and potentially a robotic arm. In a restricted area such as the OR, it can be uncomfortable for the surgical team as they have to be aware of the material and not obstruct the line of sight of the optical tracker. Further work is required to address this issue.

5 Conclusion

This work introduces and evaluates a contactless registration method adapted to featureless surfaces as fibula using a structured-light scanner to implement CAS for mandibular reconstruction with fibula free flap. The proposed method aims to reduce the registration process's invasiveness, user dependency, and time. Our results show that our contactless method is precise enough for surgery application while not using traditional anchored markers and is effective in terms of time. More validations are required and cadaver experiments are planned. Further research is required to investigate the benefit-cost ratio and final time-saving of our method compared to conventional procedures. Overall, we believe that the work presented in this paper is an important step towards providing assistance during fibula osteotomies for mandibular reconstruction and potentially even other orthopedic surgical interventions.

6 Declarations

Ethical standard Written informed consent was obtained from all individual participants before study commencement. All procedures performed in our study were in accordance with the 1964 Helsinki declaration and its later amendments. Institutional review and approval were not required due to the non-invasive nature of our study.

Conflict of interest The authors declare that they have no conflict of interest.

Acknowledgements This work was supported in part by the French National Agency for Research (Agence Nationale pour la Recherche, ANR) within the Investissements d'Avenir Program (Labex CAMI, ANR-11-LABX0004, Labex NUMEV, ANR-10-LABX-20), and by the ROBOTEX 2.0 (Grants ROBOTEX ANR-10-EQPX-44-01 and TIRREX ANR-21-ESRE-0015)

References

[1] D. A. Hidalgo. Fibula free flap: a new method of mandible reconstruction. Plast Reconstr Surg, 84(1):71–79, 1989.

[2] K. E. Blackwell, M. T. Brown, and D. Gonzalez. Overcoming the learning curve in microvascular head and neck reconstruction. Archives of Otolaryngology - Head and Neck Surgery, 123(12):1332–1335, 1997.

[3] Niklas Rommel, Marco Rainer Kesting, Nils Hagen Rohleder, Florian Martin Josef Bauer, Klaus-Dietrich Wolff, and Jochen Weitz. Mandible reconstruction with free fibula flaps: Outcome of a cost-effective individual planning concept compared with virtual surgical planning. Journal of Cranio-Maxillofacial Surgery, 45(8):1246–1250, 2017.

[4] Wen Fan, Yifei Dai, and Gérard Giordano. CAOS TKA provides improved functional outcomes compared to conventional TKA. In CAOS 2020. The 20th Annual Meeting of the International Society for Computer Assisted Orthopaedic Surgery, pages 74–69, 2020.

[5] X.-F. Shan, H.-M. Chen, J. Liang, J.-W. Huang, L. Zhang, Z.-G. Cai, and Chuanbin Guo. Surgical navigation-assisted mandibular reconstruction with fibula flaps. International Journal of Oral and Maxillofacial Surgery, 45(4):448–453, 2016.

[6] Peng Li, Ming Xuan, Chuhang Liao, Wei Tang, Xiao-yi Wang, Weidong Tian, and Jie Long. Application of intraoperative navigation for the reconstruction of mandibular defects with microvascular fibular flaps-preliminary clinical experiences. Journal of Craniofacial Surgery, 27(3):751–755, 2016.

[7] Albert H. Chao, Katie Weimer, Joerg Raczkowsky, Yaokun Zhang, Mirko Kunze, Dianna Cody, Jesse C. Selber, Matthew M. Hanasono, and Roman J. Skoracki. Pre-programmed robotic osteotomies for fibula free flap mandible reconstruction: A preclinical investigation: Robotic osteotomies of fibula free flaps. Microsurgery, 36(3):246–249, 2016.

[8] Jian-Hua Zhu, Jiang Deng, Xiao-Jing Liu, Jing Wang, Yu-Xing Guo, and Chuan-Bin Guo. Prospects of robot-assisted mandibular reconstruction with fibula flap: Comparison with a computer-assisted navigation system and freehand technique. J reconstr Microsurg, 32(9):661–669, 2016.

[9] Marie de Boutray, Joao Cavalcanti Santos, Adrien Bourgeade, Michael Ohayon, Pierre-Emmanuel Chammas, Renaud Garrel, Philippe Poignet, and Nabil Zemiti. Fibular registration using surface matching in navigation-guided osteotomies: a proof of concept study on 3d-printed models. Int J Comput Assist Radiol Surg, 17(7):1321–1331, 2022.

[10] Jürgen Hoffmann, Carsten Westendorff, Christoph Leitner, Dirk Bartz, and Siegmar Reinert. Validation of 3d-laser surface registration for image-guided cranio-maxillofacial surgery. Journal of Cranio-Maxillofacial Surgery, 33(1):13–18, 2005.

[11] Salaheddine Sta, Jérôme Ogor, Hoel Letissier, Eric Stindel, Chafiaa Hamitouche, and Guillaume Dardenne. Towards markerless computer assisted surgery: Application to total knee arthroplasty. Int J Med Robot, 2021.

[12] P. M. B. Torres, P. J. S. Gonçalves, and J. M. M. Martins. Robotic system navigation developed for hip resurfacing prosthesis surgery. In Manfred Husty and Michael Hofbaur, editors, New Trends in Medical and Service Robots, volume 48, pages 173–183. Springer International Publishing, 2018. Series Title: Mechanisms and Machine Science.

[13] Ikenna Enebuse, Mathias Foo, Babul Salam Ksm Kader Ibrahim, Hafiz Ahmed, Fhon Supmak, and Odongo Steven Eyobu. A comparative review of hand-eye calibration techniques for vision guided robots. IEEE Access, 9:113143–113155, 2021.

[14] Svenja Kahn, Dominik Haumann, and Volker Willert. Hand-eye calibration with a depth camera: 2d or 3d? In 2014 International Conference on

Computer Vision Theory and Applications (VISAPP), volume 3, pages 481–489, 2014.

[15] Lénaïc Cuau. Fast and automatic optical 3d cameras calibration for contactless surface registration in computer assisted surgery. In 2022 11th Conference on New Technologies for Computer and Robot Assisted Surgery, 2022.

[16] Lixin Yang, Qixin Cao, Minjie Lin, Haoruo Zhang, and Zhuoming Ma. Robotic hand-eye calibration with depth camera: A sphere model approach. In 2018 4th International Conference on Control, Automation and Robotics (ICCAR), pages 104–110. IEEE, 2018.

[17] Zhengyou Zhang. Iterative point matching for registration of free-form curves and surfaces. Int J Comput Vision, 13(2):119–152, 1994.

[18] Ziv Yaniv. Which pivot calibration? In Robert J. Webster and Ziv R. Yaniv, editors, SPIE Medical Imaging, page 941527, 2015.

[19] Charles Ruizhongtai Qi, Hao Su, Kaichun Mo, and Leonidas J. Guibas. Pointnet: Deep learning on point sets for 3d classification and segmentation. CoRR, abs/1612.00593, 2016.

[20] Andriy Myronenko and Xubo Song. Point set registration: Coherent point drift. IEEE Transactions on Pattern Analysis and Machine Intelligence, 32(12):2262–2275, 2010.

[21] A. Segal, D. Haehnel, and S. Thrun. Generalized-ICP. In Robotics: Science and Systems V. Robotics: Science and Systems Foundation, 2009.

[22] Jiaolong Yang, Hongdong Li, and Yunde Jia. Go-ICP: Solving 3d registration efficiently and globally optimally. In 2013 IEEE International Conference on Computer Vision, pages 1457–1464. IEEE, 2013.

[23] R. Pellini, G. Mercante, and G. Spriano. Step-by-step mandibular reconstruction with free fibula flap modelling. Acta Otorhinolaryngol Ital, 32(6):405–409, 2012.